

Applying Two Controller Schemes to Improve Input Tracking and Noise Reduction in DC-DC converters

Abstract. The compensation of the sharp jumping in the input voltage of the DC-DC converters; buck and boost has been investigated in this paper. A combined averaging and linearization techniques have been utilized to generate a mathematical model for each type of DC-DC converters. Two control schemes, Feedback and Feedforward controllers, have been applied in the developed model. The MATLAB/SIMULINK 2015a software has been used in order to demonstrate more realistic model which include some parasitic parameters. The simulation results show that using two degree of freedom controllers is better than the one with only feedback controller. The Disturbance rejection and input tracking were improved for all DC-DC converter types under several conditions.

Streszczenie. Zbadano możliwości kompensacji skoków napięcia na wejściu przekształtnika DC-DC typu buck and boost. Wyniki symulacji wykazały że użycie kontrolerów o dwóch stopniach swobody dało najlepsze rezultaty we wszystkich typach badanych przekształtników. **Zastosowanie układu dwóch kontrolerów w przekształtniku DC-DC w celu poprawy śledzenia sygnały wejścia I redukcji szumów.**

Keywords: Buck Converter, Boost Converter, Feedforward Controller, Feedback Controller.

Słowa kluczowe: przekształtniki typu boost I buck, sterowniki sprzężenia zwrotnego.

Introduction

Many factors affect considering the applications in the market such as; cost, efficiency, size and complexity. DC-DC converters such as; buck, boost and buck-boost are widely used in industry. Transferring energy from source to the load and vice versa can be improved using DC-DC converters. The source can be a battery, AC grid, photovoltaic system (PV) or different types of AC generators and the load can be AC/DC machines.

DC-DC converters are used in many power system applications such as; DC-micro grid, hybrid vehicles, and photovoltaic system. The efficiency of the system can be improved by adding a controller [1, 2]. The DC micro-grid power system is one of the systems that uses all types of converters. The sources of DC power in such grid are either PV cells or battery modules. For high power application two or more sources can be used to supply grid.

Sudden jumps in the input of DC-DC choppers can occur during the process of switching between sources. Shutting down of whole system is not an option, and one failing unit is enough to create a sudden jump in the input of the DC chopper [3]. Very well-designed feedback controller can handle the smooth disturbance in the input but not the fast one. The feedforward controller sounds promising to compensate the sharp deviation in the input voltage for the DC-DC converter.

In [4], the small signal mathematical model has been used to design the input voltage feed-forward controller, which was applied on a two-switch Buck-Boost (TSBB). The authors concluded that, by using this technique the switching process became easier and the unstable response in the output voltage due to the disturbance in the input voltage has been reduced.

In [5], the author presented a method that can estimate the input voltage and the load without measuring the actual quantities. In his work, the small signal model for the single phase boost rectifier has been developed, assuming that there is no variation in the switching frequency. The feed-forward controller connects to the duty cycle directly without waiting any signal from the output, which makes it very fast comparing with the feedback controller. Therefore, the duty cycle can be modified very quickly by providing the estimated input voltage and the load variation to the feed-forward controller. As a result of this work, the output voltage response showed a good improvement to

compensate the disturbance that caused by the changes in the reference voltage and the load.

In [6], the sliding mode controller was applied on DC-DC converter. The input voltage and the load variation were considered as the main problem in this work. The adaptive feed-forward controller and feedback controller have been used to eliminate the variation of the switching frequency.

Since the grid impedance changes during normal power system conditions, the authors in [7] presented an adaptive control system that used online grid impedance measurements. The stability of the grid-connected inverter depends on the grid impedance, which has a time-varying nature. Thus, the measurements of this impedance value become necessary. For the measurements the impulse response analysis method has been used, while the Routh-Hurwitz stability analysis approach has been used to predict the gain of the controller.

Using a new identification technique as in [8], presented an outstanding result in rejecting the disturbances even with variables parameters of the model. The small signal model has been developed to demonstrate the boost converter, which was used as a typical platform, and then feed forward controller has been designed based on Nevanlinna–Pick interpolation method with insert weighting function to eliminate the output deviation dramatically. Ultimately, identification technique has been used to make the system withstand against the load and the parameters variation. So, we were motivated by this work to apply the Nevanlinna–Pick interpolation method on different types of converters by replacing the weighting function by optimal automated feed forward gain, as we will see later, and minimize the order of the controller from second to first [9].

In this paper, four sections are introduced. The first section presents the background and the literature review. The mathematical model development of buck and boost DC-DC converters circuits and the designing of feedback and feedforward controllers are derived and proposed in section two. Simulation results and discussion for each case of proposed system of DC-DC converters are placed in section three. Finally, section four will focus on the conclusion.

Buck and Boost Converter Modelling

Figure 1 below shows the circuit diagrams for both buck and boost converters. The switch and the diode are stationary parts of each converter, so we will introduce two

modes for each converter; each one has his own circuit. Let us define two modes of operation A and B. Mode (A): the switch will be short circuit and the diode will be open circuit. Mode (B): the switch will be open circuit and the diode will be short circuit. We assume that the switch and the diode are ideal devices.

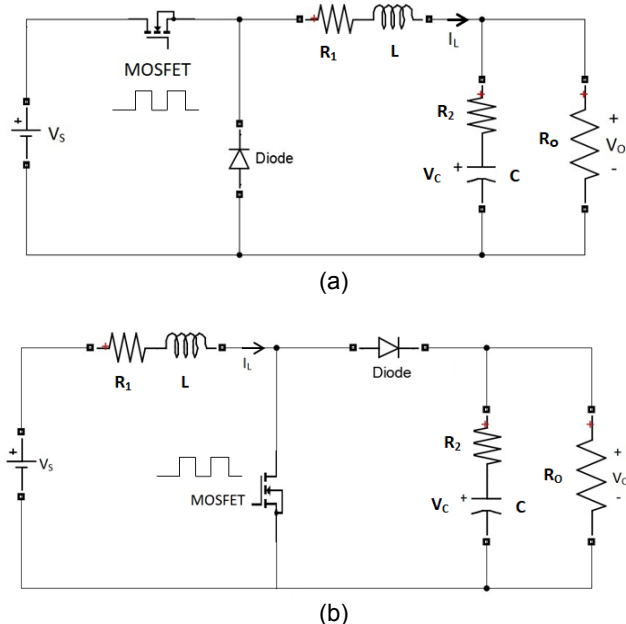


Fig.1. (a) Buck converter circuit diagram. (b) Boost converter circuit diagram.

Based on the Fig. 1, the system equations for buck and boost will be:

$$\begin{aligned} \dot{x} &= A_{bk_A}x + B_{bk_A}u & \dot{x} &= A_{bk_B}x + B_{bk_B}u \\ y &= C_{bk_A}x + D_{bk_A}u & y &= C_{bk_B}x + D_{bk_B}u \\ \dot{x} &= A_{bt_A}x + B_{bt_A}u & \dot{x} &= A_{bt_B}x + B_{bt_B}u \\ y &= C_{bt_A}x + D_{bt_A}u & y &= C_{bt_B}x + D_{bt_B}u \end{aligned}$$

where: bk: buck, bt: boost, $x = [I_L, V_C]$, $u = V_{IN}$, $y = V_O$, and

$$A_{bk_A} = \begin{bmatrix} -\left(\frac{R_1}{L} + \frac{R_0 * R_2}{L * (R_0 + R_2)}\right) & \frac{R_2}{L * (R_0 + R_2)} - \frac{1}{L} \\ \frac{1}{C} * \left(\frac{R_0}{R_0 + R_2}\right) & -\frac{1}{C} * \left(\frac{1}{R_0 + R_2}\right) \end{bmatrix} \quad B_{bk_A} = \begin{bmatrix} 1/L \\ 0 \end{bmatrix}$$

$$C_{bk_A} = \left[\frac{R_0 * R_2}{R_0 + R_2} \quad 1 - \frac{R_2}{R_0 + R_2} \right] \quad D_{bk_A} = 0$$

$$A_{bk_B} = \begin{bmatrix} -\left(\frac{R_1}{L} + \frac{R_0 * R_2}{L * (R_0 + R_2)}\right) & \frac{R_2}{L * (R_0 + R_2)} - \frac{1}{L} \\ \frac{1}{C} * \left(\frac{R_0}{R_0 + R_2}\right) & -\frac{1}{C} * \left(\frac{1}{R_0 + R_2}\right) \end{bmatrix} \quad B_{bk_B} = \begin{bmatrix} 0 \\ 0 \end{bmatrix}$$

$$C_{bk_B} = \left[\frac{R_0 * R_2}{R_0 + R_2} \quad 1 - \frac{R_2}{R_0 + R_2} \right] \quad D_{bk_B} = 0$$

$$A_{bt_A} = \begin{bmatrix} -\frac{R_1}{L} & 0 \\ 0 & -\frac{1}{C} * \left(\frac{1}{R_0 + R_2}\right) \end{bmatrix} \quad B_{bt_A} = \begin{bmatrix} 1/L \\ 0 \end{bmatrix}$$

$$C_{bt_A} = \left[0 \quad 1 - \frac{R_2}{R_0 + R_2} \right] \quad D_{bt_A} = 0$$

$$A_{bt_B} = \begin{bmatrix} -\left(\frac{R_1}{L} + \frac{R_0 * R_2}{L * (R_0 + R_2)}\right) & \frac{R_2}{L * (R_0 + R_2)} - \frac{1}{L} \\ \frac{1}{C} * \left(\frac{R_0}{R_0 + R_2}\right) & -\frac{1}{C} * \left(\frac{1}{R_0 + R_2}\right) \end{bmatrix} \quad B_{bt_B} = \begin{bmatrix} 1/L \\ 0 \end{bmatrix}$$

$$C_{bt_B} = \left[\frac{R_0 * R_2}{R_0 + R_2} \quad 1 - \frac{R_2}{R_0 + R_2} \right] \quad D_{bt_B} = 0$$

The averaged nonlinear system will be:

$$\dot{x} = (A_A * d + A_B * (1 - d))x + (B_A * d + B_B * (1 - d))u$$

$$y = (C_A * d + C_B * (1 - d))x + (D_A * d + D_B * (1 - d))u$$

where d is the duty cycle of controlled signal applied to the switch.

Applying the following steps to generate the small signal model.

- 1) Replacing each variable in the averaged system model: $\bar{u} + \hat{u}$, $x \gg \bar{x} + \hat{x}$, $\dot{x} \gg \bar{\dot{x}} + \hat{\dot{x}}$, $y \gg \bar{y} + \hat{y}$, and $y \gg \bar{y} + \hat{y}$.
- 2) Removing the steady state system from the averaged system model.
- 3) Neglecting any small variable multiplication, as example $\hat{u} * \hat{x} = 0$.

To find the equilibrium points \bar{x} then:

$$\bar{x} = (A_A * \bar{d} + A_B * (1 - \bar{d}))\bar{x} + (B_A * \bar{d} + B_B * (1 - \bar{d}))\bar{u} = 0$$

$$\bar{x} = -(\bar{d}A_A + (1 - \bar{d})A_B)^{-1}(\bar{d}B_A\bar{u} + (1 - \bar{d})B_B\bar{u})$$

The state space representation of the linear model will be:

$$\hat{\dot{x}} = \hat{A}\hat{x} + \hat{B}_1\hat{d} + \hat{B}_2\hat{u}$$

$$\hat{y} = \hat{C}\hat{x} + \hat{D}_1\hat{d} + \hat{D}_2\hat{u}$$

where:

$$\begin{aligned} \hat{A} &= A_A\bar{d} + (1 - \bar{d})A_B, & \hat{B}_1 &= (A_A - A_B)\bar{x} + (B_A - B_B)\bar{u}, \\ \hat{B}_2 &= B_A\bar{d} + (1 - \bar{d})B_B, & \hat{C} &= C_A\bar{d} + (1 - \bar{d})C_B, & \hat{D}_1 &= \\ & & & & & (C_A - C_B)\bar{x} + (D_A - D_B)\bar{u}, \text{ and } \hat{D}_2 = 0. \end{aligned}$$

The transfer function (TF) of the linear model will be:

1) The TF between \hat{d} as the input and \hat{y} as the output:

$$P_1(s) = \hat{C}(sI - \hat{A})^{-1}\hat{B}_1 + \hat{D}_1$$

2) The TF between \hat{u} as the input and \hat{y} as the output:

$$P_2(s) = \hat{C}(sI - \hat{A})^{-1}\hat{B}_2 + \hat{D}_2$$

Feedback and Feedforward Controllers Design

PI controller can be formulated as below:

$$PI(S) = K_1 + \frac{K_2}{s} \quad \text{Where: } K_1: \text{the proportional gain} \\ K_2: \text{the integral gain}$$

Figure 2 shows the feedback (FB) structure, based on the structure we have to choose the gains K_1 and K_2 to adjust the dynamic response of the system; here we can use the PID tuning MATLAB software to find out those gains.

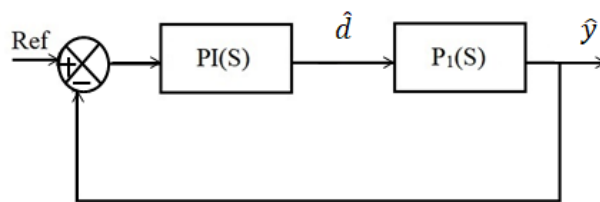


Fig.2. Feedback structure for the converters.

Using feedback controller only, d cannot be updated while the input has sudden jumps. So, the input should be controlled such that d can be updated with the input. This can be done by adding a feedforward (FF) controller to the system. The d will be continually updated about the input variation and can take action accordingly before these variation signals appear on the output. The structure that gives us this option called the FF structure as we can see in the Fig.3.

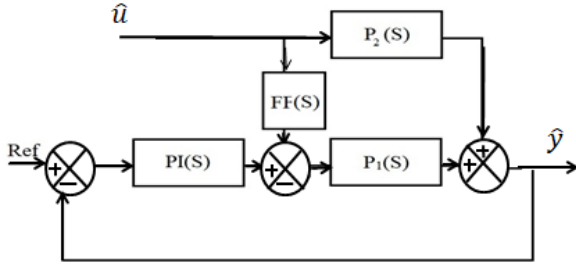


Fig.3. The FB and the FF structures for the converters.

Let us denote the feedforward controller by Q . Our goal here is to find Q , where we can minimize the deviation of the output by the variation of the input. At the same time, Q should be stable, where the finding process of the optimal Q called the model-matching problem [9,10], which is hypothetical control problem; we are going to use it during our design. We will define the minimum model-matching error as the below:

$$\alpha_{opt} = \min \|P_2 - P_1 Q\|_{\infty}$$

Based on that definition, we should diminish the α_{opt} as possible as we can to make $P_1 Q$ approximates P_2 by solving the model-matching problem using the Nevanlinna-pick interpolation method [9] to find out the optimal Q .

We are not going to introduce the general case of the Nevanlinna-pick interpolation method since our designs problem can be solved using the below two special cases:

Case 1: when the P_2/P_1 TF is stable and there are no poles on the right hand side of the poles-zeros plane, in the case, the α_{opt} will be zero and the optimal Q will be P_2/P_1 .

Case 2: when P_2/P_1 TF has one pole on the right hand side while having unstable Q is not an option as we mentioned previously, so the solution of the problem will be as below:

$$Q = \frac{P_1 - P_1(S_0)}{P_2}$$

where: Q : The optimal solution based on the Nevanlinna-pick interpolation method. S_0 : The only pole which is located on the right hand side of the pole-zero plane.

In the first case, we have seen that the α_{opt} is equal to zero, which means mathematically that there will not be any deviation on the output caused by the input variations which is a perfect solution. Although, in the second case we got the optimal solution from the Nevanlinna-pick interpolation method respective, the error is still existing and equal to $P_1(S_0)$, in that point we are going to insert a gain before the Q to minimize the error as possible as we can.

Fig.4 shows flow chart of an automated tuning method to find out the optimal feedforward controller gain K .

where:

K : FF gain, KO : optimal FF gain, E : error, EM : minimum error.

System: the TF between \hat{u} and \hat{y} , Figure 2.14.

$$P(s) = \frac{P_2(S) - P_1(S) * K * FF(S)}{1 + P_1(S) * PI(S)}$$

Disturbance: sudden jump above the equilibrium point by 10% in the input signal.

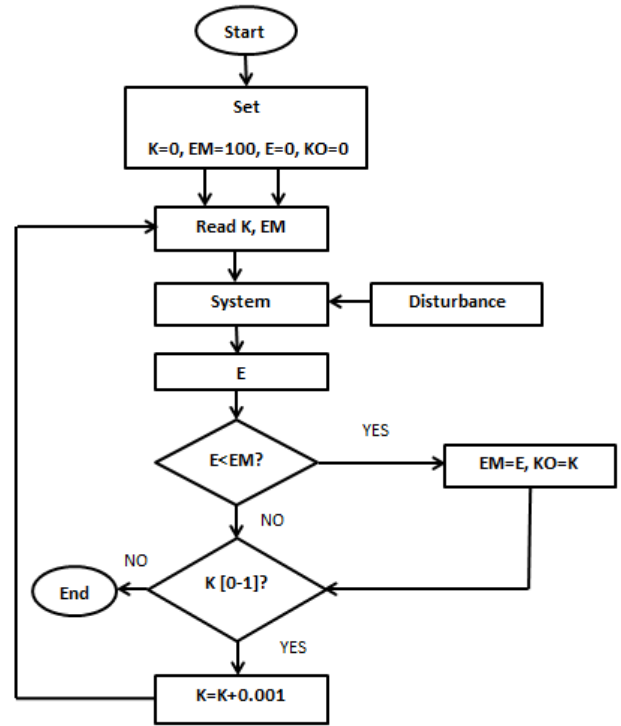


Fig.4. The flow char to find out FF controller gain K .

Simulations and Results

The structure of the controller with the real system will be shown in Fig.5. The real system in this paper will be simulated using the MATLAB/SIMULINK software. The $\hat{d}(S) = u(s) * FF(S) + E * FB(S)$. To avoid the sharp increasing or decreasing in the input signal, the TF in the Fig.6 can be used. The %error will be calculated according to the following formulas:

$$E = \frac{|V_{NOMINAL} - V_{OMAX}|}{V_{NOMINAL}} \times 100\%$$

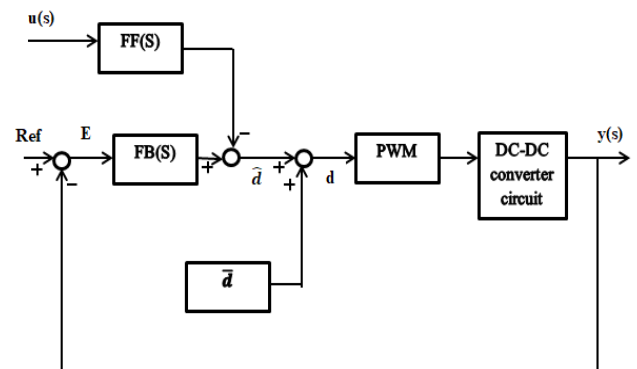


Fig.5. Block diagram of closed loop DC-DC converter with both FF and FB controllers.

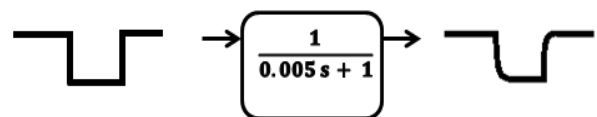


Fig.6. Disturbance signal generation.

Example 1:

In this example, the following parameters of buck circuit will be used, and then the disturbance in input by 10%

around the equilibrium point will be applied. $V_{IN} = 40$ V, $L = 3 \cdot 10^{-3}$ H, $C = 200 \cdot 10^{-6}$ F, $R_1 = 0.1$ ohm, $R_2 = 0.1$ ohm, $R_O = 25$ ohm, averaged $d = 2/3$, and $F_s = 100$ kHz.

According to the parameters given, the equilibrium points of the system will be: $\bar{I}_L = 1.0624$ A, and $\bar{V}_C = 26.5604$ V.

Driving the transfer functions of both FB and FF for the system:

The TF between \hat{d} as input and \hat{y} as the output:

$$P_1(s) = \frac{1328(s + 5e04)}{(s^2 + 265.7s + 1.667e06)}$$

The TF between \hat{u} as input and \hat{y} as the output:

$$P_2(s) = \frac{22.134(s + 5e04)}{(s^2 + 265.7s + 1.667e06)}$$

The feedback controller:

$$FB(S) = \frac{2.25}{s}$$

The feedforward controller:

$$FF(S) = \frac{22.13s + 1.107e06}{1328s + 6.64e07}$$

The dynamic response can be seen in Fig.7. Table 1 shows errors for FB and FB+FF due to 15%, 20%, 25%, and 30% input disturbance.

Table 1. percentage errors for Example 1.

Example 1	E_{FF+FB}	E_{FB}
10% disturbance	0.5156%	5.7763%
15% disturbance	1.1254%	8.5434%
20% disturbance	1.9559%	11.2329%
25% disturbance	2.9972%	13.9052%
30% disturbance	4.2401%	16.6478%

Example 2:

In this example, three parameters from specifications of example 1 are changed as follows: $V_{IN} = 20$ V, $R_O = 10$ ohm and averaged $d = 1/2$.

According to the parameters given, the equilibrium points of the system will be: $\bar{I}_L = 0.9901$ A and $\bar{V}_C = 9.9010$ V.

Driving the transfer functions of both FB and FF for the system:

The TF between \hat{d} as input and \hat{y} as the output:

$$P_1(s) = \frac{660.07(s + 5e04)}{(s^2 + 561.4s + 1.667e06)}$$

The TF between \hat{u} as input and \hat{y} as the output:

$$P_2(s) = \frac{16.502(s + 5e04)}{(s^2 + 561.4s + 1.667e06)}$$

The feedback controller:

$$FB(S) = \frac{11.8}{s}$$

The feedforward controller:

$$FF(S) = \frac{16.5s + 8.251e05}{660.1s + 3.3e07}$$

The dynamic response can be seen in Fig.8. Table 2 shows errors for FB and FB+FF due to 15%, 20%, 25%, and 30% input disturbance.

Table 2. percentage errors for Example 2.

Example 2	E_{FF+FB}	E_{FB}
10% disturbance	0.2606%	4.5300%
15% disturbance	0.5954%	6.7633%
20% disturbance	1.0609%	8.9762%
25% disturbance	1.6532%	11.1692%
30% disturbance	2.3687%	13.3430%

Example 3:

In this example, four parameters from specifications of example 1 are changed as follows: $L = 5 \cdot 10^{-3}$ H, $C = 300 \cdot 10^{-6}$ F, $R_1 = 0.2$ ohm and $R_2 = 0.2$ ohm.

According to the parameters given, the equilibrium points of the system will be: $\bar{I}_L = 1.0582$ A and $\bar{V}_C = 26.4550$ V.

Driving the transfer functions of both FB and FF for the system:

The TF between \hat{d} as input and \hat{y} as the output:

$$P_1(s) = \frac{1587.3(s + 1.667e04)}{(s^2 + 212s + 6.667e05)}$$

The TF between \hat{u} as input and \hat{y} as the output:

$$P_2(s) = \frac{26.455(s + 1.667e04)}{(s^2 + 212s + 6.667e05)}$$

The feedback controller:

$$FB(S) = \frac{2.32}{s}$$

The feedforward controller:

$$FF(S) = \frac{26.46s + 4.409e05}{1587s + 2.646e07}$$

The dynamic response can be seen in Fig.9. Table 3 shows errors for FB and FB+FF due to 15%, 20%, 25%, and 30% input disturbance.

Table 3. percentage errors for Example 3.

Example 3	E_{FF+FB}	E_{FB}
10% disturbance	0.5443%	6.9672%
15% disturbance	1.1957%	10.4093%
20% disturbance	2.0931%	13.8247%
25% disturbance	3.2316%	17.2139%
30% disturbance	4.6067%	20.5775%

Example 4:

In this example, \bar{d} from specifications of example 1 is changed to $\bar{d} = \frac{1}{2}$. The same controllers used in example 1 will be applied. The dynamic response can be seen in Fig.10. Table 4 shows errors for FB and FB+FF due to 15%, 20%, 25%, and 30% input disturbance.

Table 4. percentage errors for Example 4.

Example 4	E_{FF+FB}	E_{FB}
10% disturbance	2.5077%	5.8439%
15% disturbance	4.1701%	8.6436%
20% disturbance	6.0916%	11.3648%
25% disturbance	8.2626%	14.0597%
30% disturbance	10.6733%	16.8328%

Table 5 shows %errors for FB and FB+FF due to 15% input disturbance for different value of \bar{d} .

Table 5. percentage errors to changing \bar{d} for Example 4.

Example 4	E_{FF+FB}	E_{FB}
$\bar{d}=2/3$	1.1254%	8.5434%
$\bar{d}=1/2$	4.1701%	8.6436%
$\bar{d}=1/3$	14.6545%	11.6018%
$\bar{d}=1/4$	23.2358%	11.8353%

Example 5:

In this example, the load R_O from specifications of example 1 is replaced with DC motor, where: $R_a = 0.6$ ohm and $L_a = 0.012$ H. The same controllers used in example 1 will be applied. The dynamic response can be seen in Fig.11. Table 6 shows errors for FB and FB+FF due to 15%, 20%, 25%, and 30% input disturbance.

Table 6. percentage errors for Example 5.

Example 5	E_{FF+FB}	E_{FB}
10% disturbance	0.4653%	5.4308%
15% disturbance	1.0067%	8.0927%
20% disturbance	1.7538%	10.7098%
25% disturbance	2.1769%	13.2833%
30% disturbance	2.6762%	15.8142%

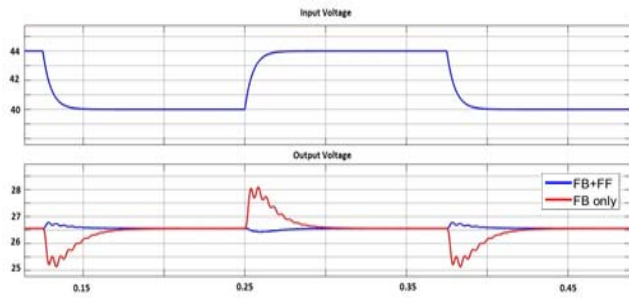


Fig.7. Dynamic response for Example 1.

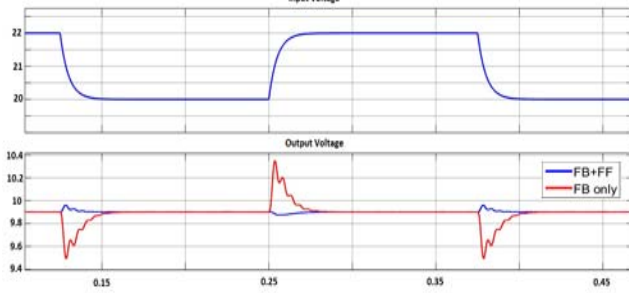


Fig.8. Dynamic response for Example 2.

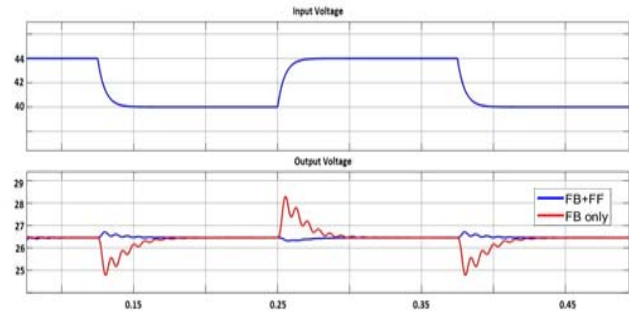


Fig.9. Dynamic response for Example 3.

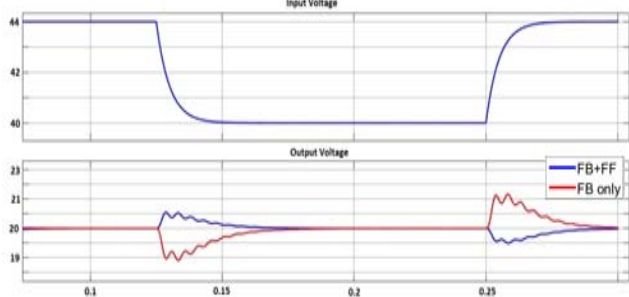


Fig.10. Dynamic response for Example 4.

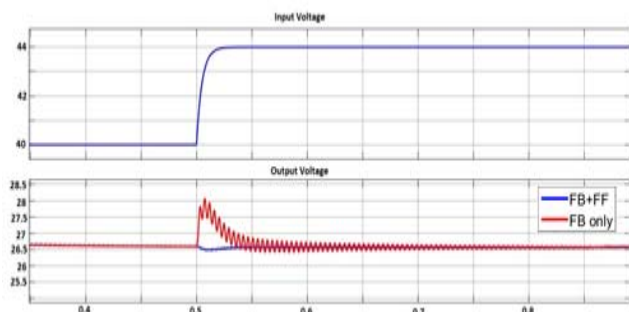


Fig.11. Dynamic response for Example 5.

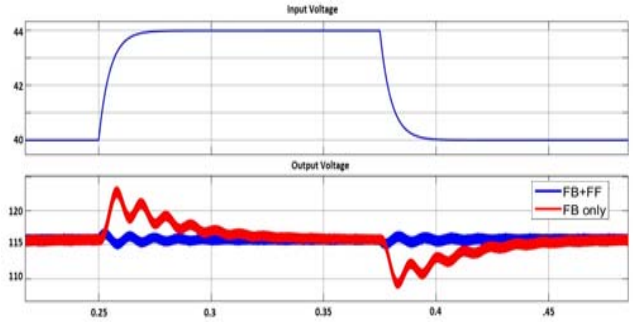


Fig.12. Dynamic response for Example 6.

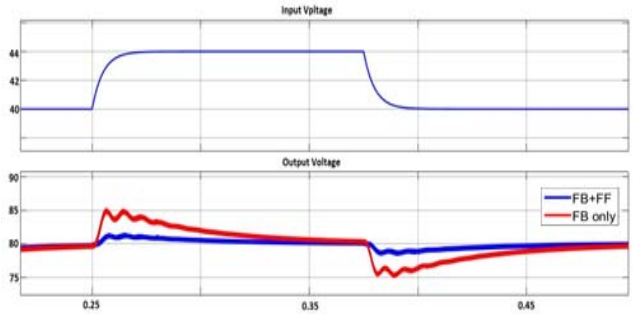


Fig.13. Dynamic response for Example 7.

Example 6:

In this example, the following parameters of boost circuit will be used, and then the disturbance in input by 10% around the equilibrium point will be applied. $V_{IN} = 40\text{ V}$, $L = 3 \cdot 10^{-3}\text{ H}$, $C = 200 \cdot 10^{-6}\text{ F}$, $R_1 = 0.1\text{ ohm}$, $R_2 = 0.1\text{ ohm}$, $R_O = 25\text{ ohm}$, averaged $d = 2/3$, and $FS = 100\text{ kHz}$. According to the parameters given, the equilibrium points of the system will be: $\bar{I}_L = 13.79\text{ A}$, and $\bar{V}_C = 114.94\text{ V}$. Driving the transfer functions of both FB and FF for the system:

The TF between \hat{d} as input and \hat{y} as the output:

$$P_1(s) = \frac{-1.3739(s + 5e04)(s - 888.9)}{(s^2 + 243.6s + 1.926e05)}$$

The TF between \hat{u} as input and \hat{y} as the output:

$$P_2(s) = \frac{11.067(s + 5e04)}{(s^2 + 243.6s + 1.926e05)}$$

The feedback controller:

$$FB(S) = \frac{0.002S + 0.2}{S}$$

The feedforward controller:

$$FF(S) = \frac{S + 1109(0.4119)}{S + 50000}$$

The dynamic response can be seen in Fig.12. Table 7 shows errors for FB and FB+FF due to 15%, 20%, 25%, and 30% input disturbance.

Table 7. percentage errors for Example 7.

Example 1	E_{FF+FB}	E_{FB}
10% disturbance	0.8129%	6.1832%
15% disturbance	1.0919%	9.1052%
20% disturbance	1.3458%	11.9722%
25% disturbance	1.5783%	14.7876%
30% disturbance	1.7925%	17.5543%

Example 7:

In this example, \bar{d} from specifications of example 6 is changed to $\bar{d} = \frac{1}{2}$. The same controllers used in example 6 will be applied. The dynamic response can be seen in Fig.13. Table 8 shows errors for FB and FB+FF due to 15%, 20%, 25%, and 30% input disturbance.

Table 8. percentage errors for Example 7.

Example 4	E_{FF+FB}	E_{FB}
10% disturbance	1.7151%	6.5245%
15% disturbance	2.4735%	9.6803%
20% disturbance	3.2131%	12.7931%
25% disturbance	3.9220%	15.8648%
30% disturbance	4.6018%	18.8971%

Table 9 shows errors for FB and FB+FF due to 15% input disturbance for different value of \bar{d} .

Table 9. percentage errors due to changing \bar{d} for Example 7.

Example 4	E_{FF+FB}	E_{FB}
$\bar{d}=2/3$	1.1254%	8.5434%
$\bar{d}=1/2$	4.1701%	8.6436%
$\bar{d}=1/3$	14.6545%	11.6018%
$\bar{d}=1/4$	23.2358%	11.8353%

From the above examples for buck and boost DC-DC converters it can be shown that: Using two degree of freedom controllers FB+FF has improved the system input tracking and decreased the percentage of error due to input disturbance. For different values of duty cycle average \bar{d} , the system still robust due to disturbance of 15% around the equilibrium point as soon as the average duty cycle is near the nominal duty cycle $\bar{d}=2/3$. The output deviation under load changes doesn't significantly increase; since using DC machine instead of resistive load has approximately same percentage errors. To achieve optimal solution due to parameters changes of DC-DC converters system, designing FB and FF controllers should be updated and the gains should be tuning also.

Conclusion

This paper proposes an optimal feedforward controller to compensate the sudden jumps in the input voltage of DC-DC converters. The results show that due to the unstable nature of the DC sources such as: PV system or the battery, the feedback controller cannot withstand against the jumps in the input. The weakness in tracking and noise rejection proposed system using FB controller only can be solved by adding FF to the system.

Dr. Mohammad A Obeidat is assistant professor in electrical power and mechatronics department at Tafila Technical University. He received his PhD in Electrical Engineering, Wayne State University, in 2013. his M.Sc degree in Electrical Engineering, Yarmouk University, Jordan, in 2006, and his B.Sc degree in Electrical Engineering, Jordan University of Science Technology, Jordan, in 1999; and He is a member of IEEE, Tau Beta Pi Honor Society, Golden Key Honor Society. He was given the honor to be a Sigma Xi member from the Board of Governor, in 2012. Mohammad Obeidat maobaidat76@gmail.com

Ali Hamad has a Master degree, School of Electrical power and control, Engineering and Applications, Tafila Technical University, Tafila, Jordan. His research interests include power lectronic, converters control and data mining in power application.

REFERENCRES

1. R. W. Erickson and D. Maksimovic, Fundamentals of Power Electronics. Norwell, MA, USA: Kluwer, 2011.
2. <https://en.wikipedia.org/wiki/Efficiency>
3. F. Misoc, M. M. Morcos, and J. Lookadoo, "Effect of DC-DC converter topologies and operation on the electrical performance of fuel cells," Electric Power Compon. Syst., vol. 38, no. 7, pp. 851–861, May 2010.
4. C. Yao, X. Ruan, W. Cao, and P. Chen, "A two-mode control scheme with input voltage feed-forward for the two-switch buck-boost DC–DC converter," IEEE Trans. Power Electron., vol. 29, no. 4, pp. 2037–2048, Apr. 2014.
5. R. Ghosh and G. Narayanan, "Generalized feedforward control of single phase PWM rectifiers using disturbance observers," IEEE Trans. Ind.Electron., vol. 54, no. 2, pp. 984–993, Apr. 2007.
6. S.-C. Tan, Y. M. Lai, C. K. Tse, and M. K. H. Cheung, "Adaptive feedforward and feedback control schemes for sliding mode controlled power converters," IEEE Trans. Power Electron., vol. 21, no. 1, pp. 182–192, Jan. 2006.
7. M. Cespedes and J. Sun, "Adaptive control of grid-connected inverters based on online grid impedance measurements," IEEE Trans. Sustainable Energy, vol. 5, no. 2, pp. 516–523, Apr. 2014.
8. Mohammad A Obeidat, "Modelling and Control of a Chopper using Feedback and Feedforward Control Schemes", IOSR Journal of Electrical and Electronics Engineering (IOSR-JEEE) ,Volume 13, Issue 5 Ver. II (Sep. – Oct. 2018), PP 06-15
9. Przemysław Orłowski, "Analysis of two-criteria optimization problem with application to automatic orders control system for inventory with long-delay supply with feedback-feedforward controller and Smith predictor", Przegląd Journal, R. 92 NR 10/2016.
10. J. C. Doyle, B. A. Francis, and A. R. Tannenbaum, Feedback Control Theory. New York, NY, USA: Macmillan, 1992.